Does β-Lactoglobulin Denaturation Occur via an Intermediate State?†

Laura D'Alfonso, Maddalena Collini, and Giancarlo Baldini*

Università degli Studi di Milano-Bicocca and INFM UdR Milano-Bicocca, P.za della Scienza, 3 I-20126 Milano, Italy

Received July 19, 2001; Revised Manuscript Received October 10, 2001

ABSTRACT: The denaturation of β-lactoglobulin (BLG) in the presence of urea and GuHCl has been investigated at different pH values with various spectroscopic techniques. The equilibrium denaturation free energy values, obtained by linearly extrapolating the data to vanishing denaturant ($\Delta G_D^{H_2O}$), are compared and discussed. The fit of the spectroscopic data monitoring the denaturation of BLG has been approached, at first, with a two-state model that describes the protein transition from the folded state (at each pH and in the absence of denaturant) to the denatured state, but in particular, along the GuHCl denaturation pathway some evidence is found of the presence of an intermediate state. Time-resolved fluorescence experiments performed on the BLG−ANS (1-anilino-8-naphthalenesulfonate) complex help to understand the results. Fluorescence polarization anisotropy (FPA) measurements accompanying the denaturation process show the presence of a fast rotational diffusion of the ANS probe, and the data are interpreted in terms of local fluctuations of a still structured tract of the denatured protein where the probe is bound.

β-Lactoglobulin (BLG),[1] a 162-residue globular protein present in large quantities in the milk of several mammals, belongs to the lipocalin superfamily. This family includes transport proteins such as the retinol binding protein, the odorant binding protein, and the major urinary protein, which all share the common structural feature of a β-barrel calyx, built from eight antiparallel β-sheets, arranged as an ideal site for hydrophobic ligands (*1*). During recent years, several investigations have been performed on bovine β-lactoglobulin to elucidate its physiological role and its folding mechanism. The spatial structure and conformation of the protein have been determined in the native state (*1*, *2*), in the acid state (*3*, *4*), and under alkaline conditions (*2*). To gain insight on the BLG folding mechanism, its denaturation process, induced by both chemical agents and temperature, has been studied by means of different techniques: ultrafiltration and dialysis (*5*−*7*), tryptophan intrinsic fluorescence (*8*, *9*), calorimetry (*10*, *11*), NMR (*12*), differential UV absorption (*13*, *14*), density (*15*), and, mainly, circular dichroism (*16*−*24*). The most recent of these works were aimed at determining whether the BLG denaturation mechanism can be adequately described by a two-state model (N ⇔ U), as suggested by circular dichroism (*24*) and NMR (*12*) measurements on the BLG acid state, or whether a more complex unfolding pathway, with different intermediate steps (*21*−*22*, *25*), is necessary. To obtain a more detailed description of the transition from the native to the denatured state, the thermodynamic parameters of the process and their dependence on the nature of the denaturant agent and on the initial state of the protein must be established. In fact, despite several denaturation studies performed on BLG, an investigation performed on a well-defined BLG variant aimed at clarifying the role of pH and the nature of the denaturant on the denaturation process is still lacking.

The aim of the present study then is that of trying to shed some light on the action of denaturing agents according to their chemical composition and of the protein electrostatic charge (dependent on solution pH) in the transition from the native to the denatured state. Two different chemical denaturing agents have been employed, urea and guanidine hydrochloride (GuHCl). The experiments have been performed in the acid state of the protein (pH 2.3), in its native state (pH 6.2), and in a condition where the protein has already undergone the so-called Tanford transition (pH 8.3; for the details of the transition see ref *26*). Furthermore, to better understand the nature of the transition process, differential UV absorption, circular dichroism, and steady-state intrinsic fluorescence have been joined by lifetime and fluorescence polarization anisotropy measurements of ANS (1-anilino-8-naphthalenesulfonate) bound to BLG. These techniques give useful information on protein conformational variations localized near the binding sites and on "effective" protein "local" dimension changes induced by the denaturing agents. BLG is reported to possess two different binding sites for the probe ANS: an "external site", in proximity of an hydrophobic patch on the protein surface, and an "internal site", located in the BLG calyx (*27*). The results have been first analyzed by means of a two-state model to describe the transition and employing the linear approximation (LEM) to express the dependence of the denaturation free energy value on denaturant concentration (*28*, *29*). Some evidence of an "ionic" intermediate state, detected at low GuHCl concentrations, is shown, and a qualitative analysis in terms of a three-state model is discussed.

† This work was supported by a grant from the Istituto Nazionale per la Fisica della Materia, Sezione B.

* Corresponding author. Tel: +390264482870. Fax: +390264482894. E-mail: giancarlo.baldini@mib.infn.it.

[1] Abbreviations: BLG, β-lactoglobulin; NMR, nuclear magnetic resonance; GuHCl, guanidine hydrochloride; ANS, 1-anilino-8-naphthalenesulfonate; CD, circular dichroism; UV, ultraviolet; FPA, fluorescence polarization anisotropy; LEM, linear extrapolation model.

10.1021/bi0115028 CCC: $22.00
Published on Web 12/05/2001

MATERIALS AND METHODS

Lyophilized bovine β-lactoglobulin, genetic variant B (Sigma Chemical Co., lot 13H7150), was dissolved in the proper buffer at the desired concentration. ANS ammonium salt was purchased from Fluka Chemical Co. Protein and dye concentrations were checked photometrically by employing the molar extinction coefficient at the absorption peak $\epsilon_{280} = 17600\ cm^{-1}\ M^{-1}$ and $\epsilon_{350} = 5000\ cm^{-1}\ M^{-1}$, respectively.

Phosphate buffers employed in the denaturant agent titration were the following: H_3PO_4/NaOH, pH 2.3, ionic strength $I = 0.007$ M; $KH_2PO_4-Na_2HPO_4$, pH 6.2, $I = 0.010$ M; $KH_2PO_4-Na_2HPO_4$/NaOH, pH 8.3, $I = 0.010$ M.

All of the reagents used in the sample preparation were of analytical grade.

The different experiments were performed in the presence of urea and GuHCl at concentrations ranging from 0 to 8 M and to 0 and 5 M, respectively. Fresh samples were prepared at each denaturant concentration by employing denaturant stock solutions at the chosen pH. In the time-resolved fluorescence measurements each denaturant concentration was prepared at least twice to check for data reproducibility. Experiments versus ionic strength were performed by employing different samples for each ionic strength value, and the ionic strength of the solution was obtained by adding to the protein solution proper aliquots of 2 M NaCl prepared in the desired buffer at the chosen pH. The BLG concentration was kept constant during each measurement and equal to about 40 μM for the differential UV absorption, near-UV circular dichroism, extrinsic ANS bound fluorescence, and time-resolved fluorescence measurements. In the far-UV circular dichroism and intrinsic fluorescence measurements the protein concentration was equal to about 5 μM. In the fluorescence experiments the ANS concentration was constant and equal to about 5 μM.

Circular dichroism measurements in both spectral regions were performed versus the time elapsed from sample preparation, from 10 min to 48 h, in the presence of different denaturant concentrations (4 and 7.5 M for urea and 2 and 4.5 M for GuHCl), and no significant change was detected in the CD spectra. Measurements were performed about 10 min after sample preparation, typically, but neither sample incubation at the different denaturant concentration nor the time elapsed from sample preparation to measure was found relevant.

GuHCl and urea stock solutions were prepared by diluting proper amounts of the denaturant powder (Sigma Chemical Co.) in the desired buffer. Due to the high hygroscopicity of these denaturants the final solution concentration was verified by measuring the solution refraction index by means of an Abbe refractometer having precision of the third decimal point and corresponding to a concentration uncertainty equal to about 0.05 M. Solution parameters, such as density, refraction index, or viscosity, were obtained from the literature (refs *30* and *31* for GuHCl) or by direct measurements. Samples prepared at acid pH employing urea stock solutions showed a small increase in the pH value (up to pH 2.8) when the denaturant concentration was increased. The absence of variation in the protein charge value during the denaturation process is taken as a key factor for the correct analysis of the experimental data, since pH variations are known to cause relevant changes in protein spectral properties (*27*). To keep the pH value (and the protein charge) constant, acid aliquots have been added to the solutions. Two different acid solutions have been employed: 1 M HCl, which leads to the presence of Cl^- ions in solution, and 85% w/w H_3PO_4, which is the same acid employed in the buffer preparation and, therefore, should not alter solution chemical properties. The resulting protein samples at pH 2.3 are labeled as "acid hcl" and "acid hpo", respectively.

Differential UV absorption measurements were performed at 25 °C in the 210−500 nm range in a 10 mm path-length quartz cell (Hellma) on samples containing increasing denaturant concentrations by employing a Perkin-Elmer Lambda 2 spectrophotometer. Spectra of both the protein and the corresponding buffer were recorded, and the latter was subtracted from the former to resolve the information concerning the BLG spectral response. The resulting spectra were normalized for protein concentration, and the difference spectra between the unperturbed state (0 M denaturant concentration) and the increasing concentration of urea and GuHCl were calculated. Particular attention was given to the differential absorption at 293 nm (averaged between 292 and 294 nm) versus denaturant concentration, where the main contribution to the absorption spectrum is due to the protein tryptophans (*13*).

Circular dichroism (CD) spectra in the near-ultraviolet (UV) at wavelengths from 240 to 350 nm and in the far-UV from 200 to 250 nm were recorded at 25 °C by a Jasco 500-A spectropolarimeter. The signal was averaged 30−40 times at each wavelength. Due to the high absorption of the denaturant at wavelengths below 205 nm, the far-UV CD signal down to 200 nm was taken only at lower urea or GuHCl concentrations (<1.5 M). These spectra were employed to monitor the secondary structure content of the samples and to follow the early steps of the denaturation process.

Steady-state measurements of BLG intrinsic fluorescence and of ANS fluorescence were performed at 25 °C with a Perkin-Elmer 650-40 spectrofluorometer. Protein tryptophans intrinsic fluorescence was excited at 295 nm and collected between 310 and 400 nm through a 305 nm long-pass filter (Andover Co.) in order to cut Rayleigh and Raman scattering. The intensity of the BLG−ANS complex fluorescence at 480 nm was detected after excitation at 350 nm using a 435 nm long-pass filter (Andover Co.). To compare results obtained at different times, a fluorescent standard sample was employed as a reference.

Fluorescence lifetimes were measured by means of a modulation fluorometer (ISS, K2). The excitation was accomplished by the 351 nm line of an argon ion laser at 80 mW power (Spectra Physics, 2025). For further details, see ref *32*. Digital data acquisition and storage were provided by the ISS-A2D ACD card inserted in a personal computer. For each data set, at least 15 logarithmically spaced frequencies were employed in the range 2−180 MHz with a cross-correlation frequency of 80 Hz. The reference sample was a solution of glycogen in bidistilled water. Both in steady-state and in dynamic measurements, the cell was thermostated at 20 ± 0.5 °C. Data fitting was accomplished by means of a least-squares minimization procedure based on Marquardt algorithm. Fluorescence lifetimes were analyzed in terms of sums of three discrete exponential components, with the

lifetime values τ_i and their corresponding fractional intensities f_i as unknown parameters, according to the expression:

$$I(t) = \sum_i x_i e^{-(t/\tau_i)} \qquad \text{and} \qquad f_i = \frac{x_i \tau_i}{\sum_i x_i \tau_i}$$

where x_i represent the preexponential factors. The lifetime of free ANS was kept constant at a value of 0.26 ns since it was found to be independent of denaturant concentration.

Concerning fluorescence polarization anisotropy (FPA) data, the protein and probe concentration values and the corresponding association constant values support the assumption that each protein molecule has at most one bound ANS (*33*). It is therefore possible to separate the FPA contributions of the ANS bound at the internal site, $r_1(t)$, where it is supposed to signal only the global protein motion, from that bound at the external site, $r_2(t)$, where, due to a lower binding rigidity, wobbling-like motions are likely, and from that of the free dye in solution, $r_F(t)$:

$$r(t) = \sum_{i=1}^{3} r_i(t) x_i e^{-(t/\tau_i)} / I(t) \qquad (1)$$

with $r_1(t)$, $r_2(t)$, and $r_F(t)$ having the expressions:

$$r_1(t) = r_0 e^{-(t/\tau_C)}$$

$$r_2(t) = r_0 (x_C e^{-(t/\tau_C)} + (1 - x_C) e^{-(t/\tau_w)})$$

$$r_3(t) = r_0 e^{-(t/\tau_3)}$$

τ_w is the probe wobbling-like time, τ_C is the overall protein rotational time with relative amplitude x_C, and τ_3 is the free dye correlation time. The measured probe rotational time in solution (at $T = 20$ °C, where $\eta = 1$ cP) and in the absence of denaturants is $\tau_{3,0} = 85$ ps. The rotational correlation time of free ANS in the presence of denaturants, τ_3, was kept fixed and equal to the product of $\tau_{3,0}$ and the relative viscosity of the sample.

RESULTS AND DISCUSSION

Two different probes have been chosen to investigate the BLG denaturation process, tryptophans (intrinsic) and ANS (extrinsic). Since the two Trp residues have different locations in the protein, one (Trp_{19}) being located at the bottom of the BLG hydrophobic calyx and the other (Trp_{61}) on the protein surface, by following the Trp response one can derive some average property change of the protein during denaturation. On the other hand, fluorescence data of the ANS probe complexed to BLG are expected to yield information on how the probe−protein interaction (binding sites and binding affinity) changes upon denaturation. The techniques employed here (near-UV circular dichroism, UV differential absorption, and UV fluorescence of Trp) monitor the protein structural changes occurring in the environment of the intrinsic probe, while steady-state and dynamic fluorescence are employed to monitor the response sensed by the extrinsic probe ANS.

BLG Denaturation Monitored by Trp Residues. Differential absorption measurements of BLG at 293 nm versus denaturant concentrations are shown in Figure 1. At first the addition

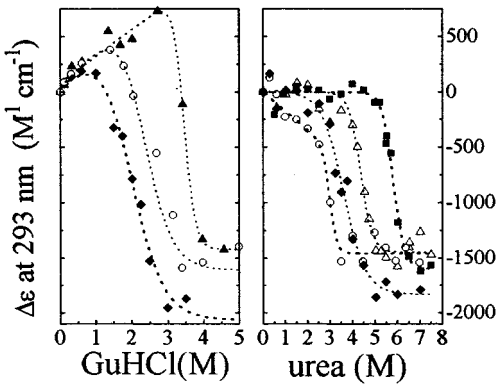

FIGURE 1: Absorption difference at 293 nm between the sample without denaturant and that containing increasing concentrations of GuHCl (left) or urea (right). The absorption spectra have been normalized for protein concentrations. The different symbols refer to different solution pH values. For GuHCl: pH 2.3, triangles; pH 6.2, circles; pH 8.3, diamonds. For urea: acid hpo, squares; acid hcl, triangles; pH 6.2, circles; pH 8.3, diamonds. Dotted lines represent data fitting by means of eq 2.

of GuHCl (left side) induces an increase of the differential absorption $\Delta\epsilon$ which, although more pronounced in the acid sample, can still be detected at pH 6.2 and also in the alkaline sample. At higher GuHCl concentrations a sharp decrease, corresponding to $\Delta\epsilon = -1500$ M^{-1} cm^{-1}, is detected. In the presence of urea at low denaturant concentration $\Delta\epsilon$ is nearly constant, whereas a decrease is detectable at higher concentrations (Figure 1, right). From the figure GuHCl appears to be a more effective denaturant agent than urea, as can be found also by the location of the midpoint concentration values of the transition from the native to the denatured state (1−2 molar shift at midpoint). For both denaturants the acid state is the most stable one against chemical denaturation. In particular, in the presence of urea the addition of HCl to fix the pH of the acid sample lowers the protein stability, as can be seen by comparing the denaturation profiles for the acid hpo and acid hcl samples. In the presence of GuHCl the protein stability is lowered by increasing pH. Concerning urea, instead, the stabilities at pH 6.2 and 8.3 become closer, with the alkaline state slightly more resistant to protein denaturation as found also with the techniques discussed below.

In Figure 2A the near-UV circular dichroism signal at 293 nm is reported. This wavelength was chosen since it corresponds to a strong signal of the tryptophans which are known to monitor the rigidity of their environment inside the protein molecule. The ellipticity values in the absence of denaturant, in agreement with previously reported data (*27*), larger for the native state ($[\Theta]_{293} \approx -100$ deg cm^2 $dmol^{-1}$), are reduced at pH 2.3 to $[\Theta]_{293} \approx -70$ deg cm^2 $dmol^{-1}$. Concerning the denaturation induced by GuHCl (see Figure 2A, left), at pH 6.2 no significant signal change occurs until the denaturation process starts. For the acid state sample, instead, at low GuHCl concentrations the CD signal is enhanced up to the value observed for the pH 6.2 sample while a similar change, though weaker, can be detected for the alkaline sample. When the denaturation is completed the CD signal is lost. In the presence of urea, on the other hand (see Figure 2A, right), the CD signal changes are due to protein denaturation only. Protein denaturation has been followed also by far-UV ellipticity at 222 nm (Figure 2B).

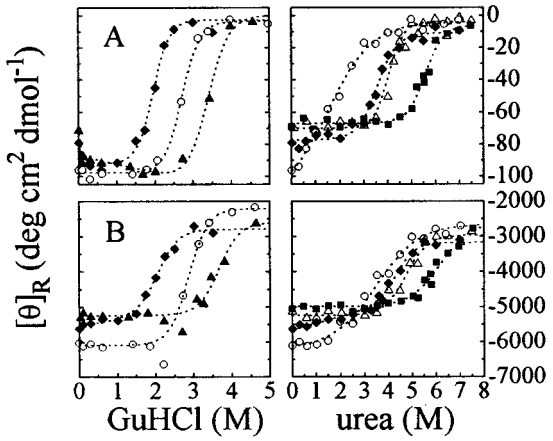

FIGURE 2: Circular dichroism signal at 293 nm (upper panels, A) and at 222 nm (lower panels, B) versus denaturant concentration (GuHCl, left, and urea, right). Symbols are as in Figure 1.

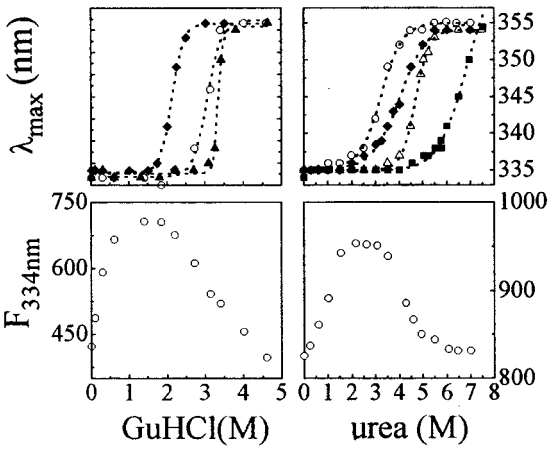

FIGURE 3: Top: Peak emission wavelength of the BLG tryptophan fluorescence spectra versus GuHCl (left) and urea (right) concentration. Bottom: pH 6.2 BLG intrinsic fluorescence emission at 334 nm versus denaturant concentration. Symbols are as in Figure 1.

The absolute value of the CD signal falls during the denaturation process, but the remaining signal found at the largest denaturant concentrations suggests that appreciably secondary structure is still present. No evidence is found for non-native secondary structure intermediates at equilibrium to the contrary of what detected by kinetic measurements (*21*−*23*, *25*).

When BLG tryptophan intrinsic fluorescence is measured versus denaturant concentration information can be obtained from the peak wavelength shift and from its intensity. The peak wavelength, reported in Figure 3, upper panels, shifts from the native state value, 335 nm, to the denatured solvent-exposed state, 355 nm. The fluorescence intensity (shown in Figure 3, lower panels, for the pH 6.2 sample) shows an initial increase at low denaturant concentrations (more pronounced for GuHCl samples), followed by a decrease attributed to the exposition of the Trp residues to the polar solvent. Denaturation profiles obtained by CD and fluorescence measurements confirm the results obtained with UV absorption.

From these data, Figures 1−3, one finds that protein stability strongly depends on pH, being larger where the net protein charge is positive (*34*). The two denaturants, although leading to the same (apparently) denatured state, are found to affect BLG stability in different ways, and in particular,

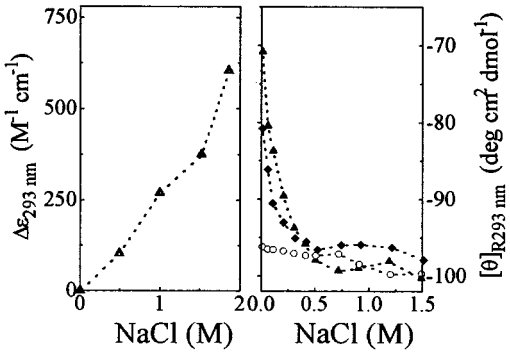

FIGURE 4: Left: Absorption difference of the pH 2.3 BLG sample in the presence of increasing amounts of NaCl. Right: CD signal at 293 nm of BLG samples in the presence of increasing amounts of NaCl. Symbols are as in Figure 1.

the pH dependence of the results suggests an electrostatic component in the interaction of GuHCl with the protein. The observed spectral properties at low GuHCl concentration suggest the onset of a conformational change opposite to that induced by denaturation. Furthermore, in the case of urea solutions, when HCl is present, the Cl^- ion is found to decrease protein stability. To test the role of Cl^- ions on protein conformation, we have performed a spectroscopic investigation on BLG samples in the presence of increasing amounts of NaCl. The data show (see Figure 4) that the effect of addition of NaCl is similar to the addition of GuHCl (at molarity lower than 2; see Figures 1 and 2). In particular, near-UV CD data (Figure 4, right) show that both NaCl and GuHCl induce an increase of the rigidity of the Trp environment. The $\Delta\epsilon_{293nm}$ increase of BLG versus salt concentration at pH 2.3 (Figure 4, left) can be related to a higher protection against solvent exposure. Far-UV CD data show that the BLG secondary structure remains unchanged in this range of salt concentrations (data not shown). Furthermore, the Trp fluorescence intensity initial increase versus GuHCl (Figure 3, lower panels) suggests a change of the environment of the inner Trp. The suppression of the outer Trp quenching (*9*) should play a minor role since the fluorescence intensity increase is not accompanied by a red shift in the peak emission wavelength, a typical result of Trp emission when transferred to an aqueous environment.

BLG Denaturation Monitored by Bound ANS. Previous fluorescence studies (*27*, *33*) have shown that ANS bound to BLG has a double exponential decay, which have suggested the presence of two binding sites with different exposure to the solvent. As reported (*27*) the two sites have the same occupancy probability since very close (20% of difference at most) binding affinities for ANS were found over a wide range of pH and ionic strength conditions. It appears of interest to study how the lifetime values can monitor the denaturation process. It was found that at both low and high denaturant concentrations and for all the investigated samples, bound ANS retains its double exponential decay as shown in Figure 5. This is taken as a clear evidence that the two distinct binding modes, found for ANS in native BLG (*27*), persist during denaturation. Large decreases, about 50%, are observed for both of the lifetime values (τ_1, the longer, and τ_2, the shorter) versus denaturant at each pH value. The differences reside in the initial slope of the denaturation profile: in particular, the longer lifetime is shown to decrease more slowly in the pH 2.3 state than

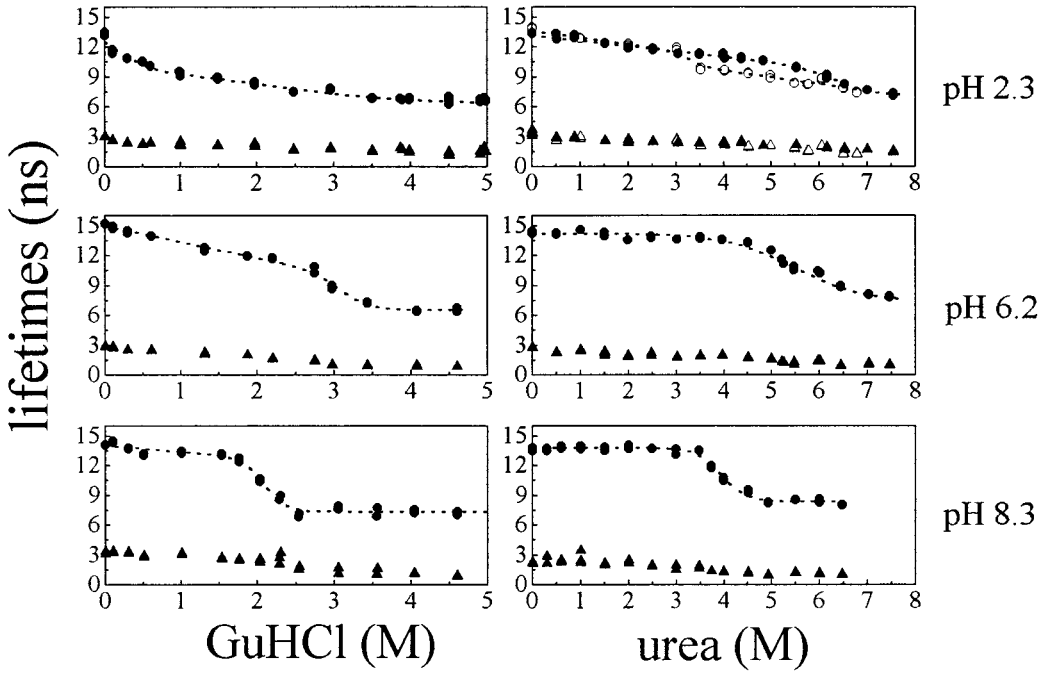

FIGURE 5: ANS bound to BLG lifetimes versus denaturant concentration (GuHCl, left, and urea, right). In the panels are shown both the longer (circles) and the shorter (triangles) bound ANS lifetimes. For urea: acid hpo, filled symbols; acid hcl, open symbols. Dotted lines are the best fitting curves according to eq 2.

in both the pH 8.3 and the pH 6.2 samples. At high denaturant concentrations two distinct lifetimes, τ_1 around 6−7 ns and τ_2 around 1 ns, are found, independent of pH and denaturant nature (urea and GuHCl), thereby suggesting similar protein unfolded states in the two instances. The presence of the two lifetimes at these extreme conditions indicates that the ANS environment maintains some peculiarity of the native state even when BLG is largely unfolded as inferred from far-UV CD data. In agreement with some earlier findings, these "still structured" regions should be located in the proximity of the disulfide bridges, which are known to persist even in the denatured conformation and which confer some constraints to the unfolded state by making it a cross-linked random coil (*35*). More in detail, one of the two disulfide bridges of BLG (Cys_{106}−Cys_{119}) connects the βG and βH strands inside the BLG hydrophobic calyx where ANS is supposed to bind. In particular, this GH strand is shown to be both the first strand to fold and the most resistant versus protein unfolding (*25*), thereby preserving part of the protein hydrophobic core to which ANS is bound.

From the denaturation profiles of ANS lifetime (Figure 5) the transition midpoint appears to depend on pH and denaturant nature, in agreement with other findings (see Figures 1−3). Again, at low GuHCl concentration the ANS lifetime has an initial drop which is much more pronounced than that with urea. The lifetime decrease can again be correlated with that found in the presence of NaCl as previously reported (*27*). In particular, according to a procedure previously described (*27*), by combining lifetime and fractional intensities, one can extract the values of the ANS to BLG binding constants. We notice that upon denaturation the binding affinity of ANS for the internal site drops by about 2 kcal/mol at pH 2.3 and about 1 kcal/mol at pH 6.2 and 8.3 from the values of 4.8, 3.5, and 3.9 kcal/mol, respectively, in the absence of denaturant. The binding

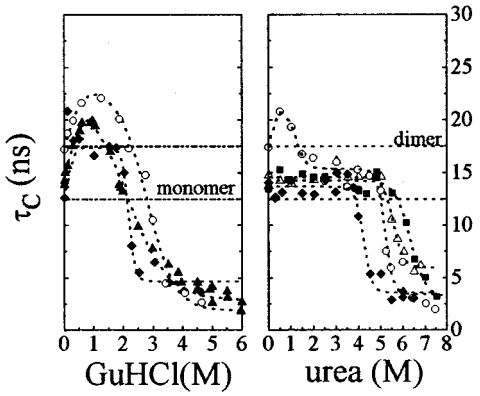

FIGURE 6: Longer ANS bound to BLG rotational correlation time versus denaturant concentration (GuHCl, left, and urea, right). Values reported in the figure are obtained by fitting with the eq 1 FPA curves. Symbols are as in Figure 1. Dot-dashed lines enlighten the rotational correlation time values for ANS bound to the BLG dimer and monomer.

affinities for the external site versus denaturant are mainly affected by ionic screening and do not show denaturation steps. This agrees with the expectation that the external site has a nonspecific (i.e., mainly electrostatic) interaction with ANS, contrary to that of the internal site whose nature is certainly affected by structural changes of the protein.

Interesting information on the BLG global conformation during the denaturation process can be gained by measuring the FPA of the bound probe ANS. The experimental data have been fitted with eq 1, as described in the Materials and Methods section, and the rotational correlation times obtained from the fitting procedures are reported versus GuHCl (left) or urea (right) concentration in Figure 6. From the FPA data it is then possible to learn about the aggregation degree of BLG. In the absence of denaturants BLG aggregation depends on pH: BLG is found to be essentially monomeric ($\tau_C \approx 12$ ns) at pH 2.3 and 8.3 and at the concentrations

Table 1: Thermodynamic Parameter Values As Deduced from the Different Experimental Data Fitting Performed by Employing Eq 2[a]

	GuHCl								
	pH 2.3			pH 6.2			pH 8.3		
techniques	m	C_{mid}	$\Delta G_D^{H_2O}$	m	C_{mid}	$\Delta G_D^{H_2O}$	m	C_{mid}	$\Delta G_D^{H_2O}$
diff abs	3.9	3.4	13.4	2.5	2.7	8.4	3.2	2.3	7.6
CD 222	3.8	3.5	13.0	3.3	2.9	9.5	3.0	2.0	5.9
CD 293	4.4	3.5	15.2	2.5	2.7	6.9	3.4	2.0	6.9
λ_{max}	4.6	3.3	15.2	3.2	3.0	6.7	3.9	2.1	8.3
mean	4.2 ± 0.4	3.4 ± 0.1	14.2 ± 1.2	2.9 ± 0.4	2.8 ± 0.2	7.9 ± 1.3	3.4 ± 0.4	2.1 ± 0.1	7.2 ± 1.0

	urea											
	acid hpo			acid hcl			pH 6.2			pH 8.3		
techniques	m	C_{mid}	$\Delta G_D^{H_2O}$	m	C_{mid}	$\Delta G_D^{H_2O}$	m	C_{mid}	$\Delta G_D^{H_2O}$	m	C_{mid}	$\Delta G_D^{H_2O}$
diff abs	1.6	5.8	10.8	1.5	4.4	7.9	0.9	4.1	3.7	1.1	3.5	4.0
CD 222	1.7	5.5	9.6	1.3	4.7	6.0	0.7	3.5	2.3	1.5	4.4	6.4
CD 293	2.2	5.7	12.6	1.8	4.3	7.7	0.6	2.1	1.4	1.4	3.6	5.0
λ_{max}	1.3	6.4	8.3	2.0	4.7	9.5	1.3	3.2	4.3	1.0	4.0	4.1
mean	1.7 ± 0.4	5.85 ± 0.3	10.3 ± 1.8	1.6 ± 0.3	4.5 ± 0.2	7.8 ± 1.4	0.9 ± 0.3	3.2 ± 0.8	2.9 ± 1.3	1.2 ± 0.2	3.9 ± 0.4	4.9 ± 1.1

[a] In the table are reported the value of the m parameter (kcal mol^{-1} M^{-1}), the transition midpoint concentration, C_{mid} (M), and the conformational stability of the protein, $\Delta G_D^{H_2O}$ (kcal mol^{-1}) obtained from the denaturation profiles measured with the different spectroscopic techniques.

used here, while it is mainly in its dimeric form ($\tau_C \approx 17$ ns) at pH 6.2. The rotational correlation time increases at low GuHCl concentration up to values larger than those found for a BLG dimer, suggesting a higher aggregation degree. The same behavior has been observed in the presence of urea at pH 6.2. Aggregation, however, is lost upon unfolding since the value of the rotational correlation time decreases versus denaturant concentration down to values much shorter than that expected for the monomer. The value of the correlation time at high denaturant concentration, $\tau_C \approx 3-4$ ns, is very likely to be due to a segmental motion of the residual structured regions of the protein where ANS can still bind, as already discussed. A rotational time of 3−4 ns, if attributed to a rigid BLG, would lead to the absurd conclusion that the denatured state is more compact than the native one. In fact, if BLG retained its globular shape during denaturation, the observed 3-fold decrease of the rotational correlation time would mean a protein radius $1/3^{1/3} \approx 0.7$ times smaller than that of the monomer, since the rotational correlation time is proportional to protein volume. Elongated (ellipsoidal) conformations would lead to rotational correlation times larger than those observed, whatever the chosen axial ratio, and therefore they can be ruled out. Preliminary small-angle X-ray scattering experiments on BLG solutions in the presence of GuHCl and urea support our data on ANS fluorescence. In fact, the BLG radius of gyration derived at high denaturant concentration gives a value corresponding to a mere 2-fold increase of the protein volume (P. Mariani and F. Spinozzi, personal communication), indicating that the denatured protein, though somehow expanded, still retains a fairly compact conformation. Further refinements on this analysis yielding information on the number of the rigid portions of the protein and their average dimensions will be the subject of a forthcoming paper.

Thermodynamic Data Analysis. The denaturation profiles can be analyzed by assuming a two-state model which describes the transition from the native to the denatured state. Given an observable ζ, the formalism generally used states that $\zeta = \zeta_N f_N + \zeta_D f_D$, where ζ_N and ζ_D are the values corresponding to the native and to the denatured state, respectively, and f_N and f_D represent the relative protein fractions, respectively, $f_N + f_D = 1$. The denaturation equilibrium constant, K_D, and the corresponding free energy, ΔG_D, are given by the equation:

$$K_D = e^{-\Delta G_D/RT} = \frac{f_D}{f_N} = \frac{(\zeta - \zeta_N)}{(\zeta_D - \zeta)}$$

The value of ΔG_D at zero denaturant concentration, $\Delta G_D^{H_2O}$, can be derived from the widely used linear extrapolation model (LEM) obtaining $\Delta G_D = \Delta G_D^{H_2O} - mC_{den}$ with $\Delta G_D^{H_2O} = mC_{mid}$, where C_{den} and C_{mid} are the denaturant and the transition midpoint concentrations, respectively.

Accordingly, the denaturation profiles were analyzed by employing the equation:

$$\zeta = \frac{\zeta_N + \zeta_D e^{-\Delta G_D/RT}}{1 + e^{-\Delta G_D/RT}} = \frac{\zeta_N + \zeta_D e^{-(\Delta G_D^{H_2O} - mC_{den})/RT}}{1 + e^{-(\Delta G_D^{H_2O} - mC_{den})/RT}} \quad (2)$$

The fitting curves, obtained by adding, when necessary, proper baselines to the model, are shown in Figures 1−3, 5, and 6 as dotted lines. The values of m, C_{mid}, and $\Delta G_D^{H_2O}$ are reported in Table 1 for the different spectroscopic techniques. The data in Table 1 show that in the presence of GuHCl the C_{mid} values are lower and the slopes m and the $\Delta G_D^{H_2O}$ values are larger than in the presence of urea. These findings are in agreement with the assumption that ionic denaturants are more effective (*28*, *29*, *36*), probably due to the higher propensity of GuHCl to form hydrogen bonds with the protein (*15*, *37*). The protein stability dependence on pH agrees with the visual inspection of the denaturation profiles discussed above. Furthermore, by comparing the two pH 2.3 samples in the presence of urea, it is found that the Cl^- ion lowers the stability of the protein structure since ΔG changes from about 10 to about 8 kcal/mol.

The values of C_{mid} found here at pH 6.2 are substantially in agreement with what reported by Creamer and by Galani et al. (*9*, *14*) for BLG at pH 6.7 (sodium phosphate buffer, about 100 mM ionic strength) and pH 7 (sodium phosphate buffer, about 50 mM ionic strength and 25 °C), respectively. Higher m, and therefore $\Delta G_D^{H_2O}$ values, instead, could be

attributed to the different pH of the examined samples. The value of $\Delta G_D^{H_2O}$ found in the present work at pH 2.3 acid hcl is in agreement with that measured by Lapanje and coworkers (*13*, *38*), who found, for a solution of a mixture of BLG A and B genetic variants (pH 2, glycine−HCl buffer, 37 °C), a value of 8.8 (±1.3) kcal/mol, and by Ragona et al. (*12*), who found, from NMR measurements on BLG (pH 2.1, phosphate buffer, 37 °C), a value of 8.3 (±0.9) kcal/mol. The experiments of Galani et al. (*14*) support the findings for this sample in the urea-induced denaturation since at pH 2.6 in a glycine buffer at 25 °C they found a value of m equal to 1.8 (±0.1) kcal/(mol M), a C_{mid} value equal to 4.6 M, and a $\Delta G_D^{H_2O}$ value of 8.1 (±0.5). The different values of the thermodynamic parameters could perhaps be ascribed to their different genetic variants or to the different protein purification procedures.

The denaturation profiles obtained with urea are well described by a two-state model. On the other hand, it has been shown that in the case of GuHCl the use of a baseline was necessary in order to obtain a satisfactory description of the experimental data at low denaturant concentration. In this region the spectroscopic properties of BLG (Figures 1−3) display a trend opposite to that observed when full denaturation takes place. A similar behavior has also been detected when NaCl is added to BLG solutions. This similarity suggests that BLG in the presence of a denaturing ionic agent, such as GuHCl, may go through an intermediate ionic state I before reaching the full denatured state. The I state, although characterized by a secondary structure very close to that of the native state, shows a larger rigidity of the tryptophan environment (Figures 1 and 2) whose difference from that of the corresponding native state depends on the number of charges on the protein. This intermediate state does not seem to be directly related to the denaturation process per se, but it is rather attributed to electrostatic effects involving the charge on the protein and the ions in solution. In fact, the transition to I is more evident the more the protein is charged (i.e., for pH = 2.3), since the effect of adding ions to the solutions is that of screening the electrostatic repulsion among charged residues, allowing the protein to assume a more rigid conformation. These observations suggest also that the free energy difference of denaturation from the intermediate state is larger than that from the native state, as shown in Figure 7. The existence of the I state could also explain the differences found in the denaturation free energy values for GuHCl and for urea. A three-state analysis of the thermodynamic parameters involved in the denaturation transition requires

$$K_{NI} = \frac{f_I}{f_N} = e^{-\Delta G_{NI}/RT}$$

$$K_{ID} = \frac{f_D}{f_I} = e^{-\Delta G_{ID}/RT}$$

and

$$\Delta G_D = \Delta G_{NI} + \Delta G_{ID}$$

where now $f_N + f_I + f_D = 1$, $\zeta = \zeta_N f_N + \zeta_I f_I + \zeta_D f_D$, and ζ_I is the value assumed by the observable ζ in the intermediate state with fraction f_I. The fit of protein denaturation data is obtained by the equation:

$$\zeta = \frac{\zeta_N - \zeta_I}{1 + e^{-\Delta G_{NI}/RT} + e^{-\Delta G_D/RT}} + \frac{(\zeta_D - \zeta_I)e^{-\Delta G_D/RT}}{1 + e^{-\Delta G_{NI}/RT} + e^{-\Delta G_D/RT}} + \zeta_I$$

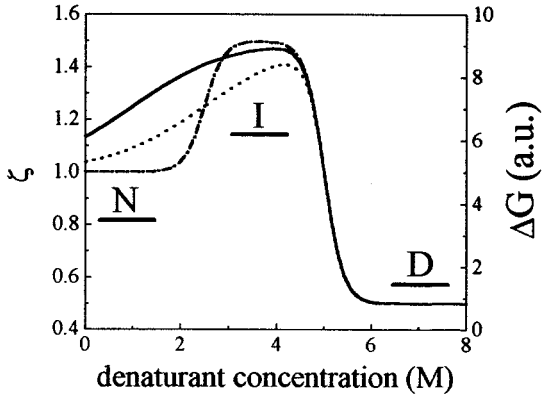

FIGURE 7: Simulations of three-state denaturation profiles obtained by varying the values of m_{NI} and C^{NI}_{mid} values: dot-dashed lines, 3.0 kcal mol^{-1} M^{-1} and 2.5 M; dotted lines, 0.6 kcal mol^{-1} M^{-1} and 2.5 M; solid lines, 0.6 kcal mol^{-1} M^{-1} and 1.0 M, respectively. The reference values assumed for the observable ζ are $\zeta_N = 1.0$, $\zeta_I = 1.5$, and $\zeta_D = 0.5$; the values of m_{ID} and C^{ID}_{mid} have been kept constant and equal to 3 kcal mol^{-1} M^{-1} and 5 M, respectively. The symbols N, I, and D refer to the native, the intermediate, and the denatured state free energy levels, respectively. The free energy right axis is in arbitrary units.

The next step is that of adopting the linear model both for ΔG_{NI} and for ΔG_{DI}, $\Delta G_{NI} = m_{NI}(C^{NI}_{mid} - C_{den})$, and $\Delta G_{ID} = m_{ID}(C^{ID}_{mid} - C_{den})$. The free energy difference for the overall process, ΔG_D, given by the sum of ΔG_{NI} and ΔG_{ID}, should be smaller than the ΔG_D value for the two-state model, since ΔG_D(two state) corresponds to ΔG_{ID}, while ΔG_{NI} is described by the baseline. Some simulations of the denaturation profiles are shown in Figure 7 at different values of the parameters controlling the native to intermediate state transition. The value of m_{NI} appears to be relevant in determining the denaturation profile at low GuHCl concentrations. In particular, only simulations with m_{NI} lower than about 0.6 kcal mol^{-1} M^{-1} allow a reasonable description of the data, while the curves are much less sensitive to C^{NI}_{mid}, a value which determines uniquely the concavity of the initial portion of the curve. Despite the qualitative character of the analysis, the curves can reproduce the UV differential absorption and near-UV CD data, which are then compatible with a three-state transition. We recall that this intermediate state may be not intrinsically related to the denaturation pathway, since not detected by urea denaturation, but rather it appears related to the ionic nature of the denaturing agent.

ACKNOWLEDGMENT

The authors acknowledge Riccardo Bonomi for participation in the early stage of the project. Thanks are due also to Paolo Mariani and Francesco Spinozzi of the Istituto di Scienze Fisiche and Istituto Nazionale per la Fisica della Materia, Università di Ancona, for preliminary results on SAXS measurements and to Henriette Molinari for helpful discussion.

REFERENCES

1. Brownlow, S., Cabral, J. H. M., Cooper, R., Flower, D. R., Yewdall, S. J., Polikarpov, I., North, A. C. T., and Sawyer, L. (1997) *Structure 5*, 481−495.
2. Qin, B. Y., Bewley, M. C., Creamer, L. K., Baker, H. M., Baker, E. N., and Jameson, G. B. (1998) *Biochemistry 37*, 14014−14023.
3. Kuwata, K., Hoshino, M., Forge, V., Era, S., Batt, C. A., and Goto, Y. (1999) *Protein Sci. 8*, 2541−2545.
4. Uhrinova, S., Smith, M. H., Jameson, G. B., Uhrin, D., Sawyer, L., and Barlow, P. N. (2000) *Biochemistry 39*, 3565−3574.
5. Warren, J. R., and Gordon, J. A. (1971) *Biochim. Biophys. Acta 229*, 216−225.
6. Špan, J., and Lapanje, S. (1973) *Biochim. Biophys. Acta 295*, 371−378.
7. Špan, J., Lenarcic, S., and Lapanje, S. (1974) *Biochim. Biophys. Acta 359*, 311−319.
8. Kaplanas, R. I., Bukolova, T. G., and Burshtein, É. A. (1975) *Mol. Biol. 9*, 795−804.
9. Creamer, L. K. (1995) *Biochemistry 34*, 7170−7176.
10. Paz Andrade, M. I., Jones, M. N., and Skinner, H. A. (1976) *Eur. J. Biochem. 66*, 127−131.
11. Lapanje, S., Lunder, M., Vlachy, V., and Skerjanc, J. (1977) *Biochim. Biophys. Acta 491*, 482−490.
12. Ragona, L., Fogolari, F., Romagnoli, S., Zetta, L., Maubois, J. L., and Molinari, H. (1999) *J. Mol. Biol. 293*, 953−969.
13. Poklar, N., Vesnaver, G., and Lapanje, S. (1993) *Biophys. Chem. 47*, 143−151.
14. Galani, D., and Apenten, R. K. O. (1999) *Food Res. Int. 32*, 93−100.
15. Poklar, N., and Lapanje, S. (1992) *Biophys. Chem. 42*, 283−290.
16. Tanford, C., and De, P. K. (1961) *J. Biol. Chem. 236*, 1711−1715.
17. Pace, C. N., and Tanford, C. (1968) *Biochemistry 7*, 198−208.
18. Green, R. F., and Pace, C. N. (1974) *J. Biol. Chem. 249*, 5388−5393.
19. Pace, C. N., and Marshall, H. F. (1980) *Arch. Biochem. Biophys. 199*, 270−276.
20. Kuwajima, K., Yamaya, H., and Sugai, S. (1996) *J. Mol. Biol. 264*, 806−822.
21. Hamada, D., and Goto, Y. (1997) *J. Mol. Biol. 269*, 479−487.
22. Arai, M., Ikura, T., Semisotnov, G. V., Kihara, H., Amemiya, Y., and Kuwajima, K. (1998) *J. Mol. Biol. 275*, 149−162.
23. Kuwata, K., Hoshino, M., Era, S., Batt, C. A., and Goto, Y. (1998) *J. Mol. Biol. 283*, 731−739.
24. Ragona, L., Confalonieri, L., Zetta, L., De Kruif, K. G., Mammi, S., Peggion, E., Longhi, R., and Molinari, H. (1999) *Biopolymers 49*, 441−450.
25. Forge, V., Hoshino, M., Kuwata, K., Arai, M., Kuwajima, K., Batt, C. A., and Goto, Y. (2000) *J. Mol. Biol. 296*, 1039−1051.
26. Tanford, C., Bunville, L. G., and Nozaki, Y. (1959) *J. Am. Chem. Soc. 81*, 4032−4035.
27. Collini, M., D'Alfonso, L., and Baldini, G. (2000) *Protein Sci. 9*, 1968−1974.
28. Pace, C. N. (1986) *Methods Enzymol. 131*, 266−280.
29. Myers, J. K., Pace, C. N., and Scholtz, J. M. (1995) *Protein Sci. 4*, 2138−2148.
30. Kawara, K., and Tanford, C. (1966) *J. Biol. Chem. 241*, 3228−3232.
31. Nozaki, Y. (1972) *Methods Enzymol. 26*, 43−50.
32. Collini, M., Chirico, G., Baldini, G., and Bianchi, M. E. (1995) *Biopolymers 36*, 211−225.
33. D'Alfonso, L., Collini, M., and Baldini, G. (1999) *Biochim. Biophys. Acta 1432*, 194−202.
34. Basch, J. J., and Timasheff, S. N. (1967) *Arch. Biochem. Biophys. 118*, 37−47.
35. Tanford, C. (1968) *Adv. Protein Chem. 23*, 121−282.
36. Castellino, F. J., and Barker, R. (1968) *Biochemistry 7*, 4135−4138.
37. Aune, K. C., and Tanford, C. (1969) *Biochemistry 8*, 4586−4590.
38. Lapanje, S., and Poklar, N. (1989) *Biophys. Chem. 34*, 155−162.

BI0115028